Eng. & Tech. Journal, Vol.28, No.14, 2010

Dynamic Failure Mode And Impact Energy Absorption of Filament-Wound Square Cross-Section Composite Tubes

Dr.Hussain J. Al-Alkawi* & Mohammad Abdul Hassan Whaib*

Received on: 28/9/2009
Accepted on: 16/2/2010

Abstract

In the present work simulation of impact response using LS-DYNA explicit finite element code is described to investigate the crash behavior and energy absorption characteristics of square glass fiber reinforced plastic tubes, subjected to impact load. Filament-wound tubes with two layers [+45º, -45º] were fabricated and tested. The experimental crushing characteristics data are compared with the obtained numerical results, showing good agreement. The effect of geometrical parameters, winding angle and the failure mode on the energy absorption characteristics are also investigated.

Keywords: Filament-wound tube, Energy absorption, LS-DYNA, Impact, Winding angle.

اسلوب الفشل الديناميكي وطاقة الصدمة الممتصة لانابيب المواد المركبة ذات المقطع المربع المصنوعة من الشعيرات الملفوقة

الخلاصة

في البحث الحالي تم اجراء محاكاة لاستجابة الصدمة باستخدام البرنامج الحاسوبي LS-DYNA، و ذالك لدراسة سلوك التحطيم و الطاقة الممتصة لانابيب ذات مقطع مربع مصنوعة من الياف الزجاج و البولستر، معرضة لحمل الصدمة. تم تصنيع انابيب بطريقة اللف و بطبقتين [+٤٥°،-٤٥°] و تم اجراء اختبار الصدمة عليها. اجريت مقارنة بين النتائج العملية و النتائج التي تم الحصول عليها من طريقة التحليل العددي حيث كان هناك توافق جيد بينهما. تم ايضا اجراء دراسة تاثير المتغيرات للشكل الهندسي للعينة و زاوية اللف و اسلوب الفشل على الطاقة الممتصة للانابيب.

* Electromechanical Engineering Department, University of Technology/ Baghdad

https://doi.org/10.30684/etj.28.14.16
2412-0758/University of Technology-Iraq, Baghdad, Iraq

Introduction

Demand for greater weight saving and crashworthiness protection has only been possible using new design concepts and employing lightweight materials. To meet these crucial factors, structures designed to withstand an axial compression started to appear in the form of thin-walled curved shells constructed from new materials such as aluminum, polymers and other composite materials [1]. Fiber-reinforced polymeric composites have gained acceptance for use in many industries including aerospace, automotive, infrastructure, and recently oil and gas. FRPs possess superior strength to weight ratios over traditional materials and their processing is well-suited to many applications [2]. When introducing new materials, such a composite, one has to consider an important design aspect, namely the crashworthiness of the material. Crashworthiness is the capability of a material in absorbing high impact energy during collision in a progressive, controlled and irreversible manner. Materials with high crashworthiness value are desired, for these materials are capable of reducing the impact force on passengers and transportation cargo [3]. Hull [4] classified three modes of failure for square-ended brittle material tubes. These three modes were Euler buckling, which was easily avoided, shell buckling and progressive folding, and brittle fracture. The brittle fracture mode was then further categorized into catastrophic failure and progressive crushing, and progressive crushing was further categorized into splaying and fragmentation. Fragmentation was characterized by crushing and then breaking off of small pieces both inside and outside of the tube. Energy absorption capability of composite wrapped aluminum tubes was investigated by Shin et al [5] under axial compressive and bending load. The effect of ply orientation under these load condition was examined. It is concluded that the best energy absorption is attained in tubes wrapped with 90º ply orientation. Mahdi et al. [6] studied experimentally and numerically the effect of the structural geometry, fiber diameter and fiber orientation on the axial collapse load of unidirectional cotton / epoxy tubes. Tubes with different diameters and fiber orientation angles were examined and tested. The initial geometric imperfections are measured using the computerized Mistral coordinate measuring machine. A limited agreement between the experimental and computational results was obtained. It was found that the load-displacement curves of the tubes are strongly dependent on the geometry configuration, the amount of energy absorbed by the tube depends on the crushing mechanism and a bigger fiber diameter provides a higher load resistance as well as higher energy absorption. Zeng et al. [7] simulated the crash behavior and energy absorption characteristics of 3D braided composite tube subjected to axial impact loading, using the explicit finite element Code LS-DYNA. The effect of geometrical and braid parameters on the energy

* Electromechanical Engineering Department, University of Technology/ Baghdad

absorption characteristics were investigated. Mamalis et al. [8] studied the crushing response and crashworthiness characteristics of thin-wall square FRP (fiber reinforced plastic) tubes that were impact tested at high compressive strain rate were compared to the response of the same tubes in static axial compressive loading. The material combination of the tested specimens was carbon fibers in the form of reinforcing woven fabric in epoxy resin, and the tested tubes were constructed trying three different laminate stacking sequences and fiber volume contents on approximately the same square cross section. Comparison of the static and dynamic crushing characteristics was made. The influence of the tube geometry (axial length, aspect ratio and wall thickness), the laminate material properties such as the fiber volume content and stacking sequence and the compressive strain rate on the compressive response, the collapse modes, the size of the peak load and the energy absorbing capability of the thin-wall tubes was extensively analyzed. . Al-Badrany [9] presented an experimental study for axial loading of AISI 5053 Aluminum alloy tubes, quasi-statically and dynamically at room temperature conditions. Tow types of specimens were used, circular and square cross-sections tubes with equal cross-sectional areas. Empirical models was proposed and compared with the well- known models. It was found that the circular cross-sections specimens absorbed the impact energy grater than the square cross-sectioned specimens, and the energy mainly depends on the configuration of the cross sections and the manners of deformation. Mamalis et al. [10] investigated the compressive properties and crushing response of square carbon FRP (fiber reinforced plastic) tubes subjected to static axial compression and impact testing by means of numerical simulation using the LS-DYNA3D explicit finite element code. A series of models was created to simulate some of the static and dynamic tests using CFRP tubes featured by the same material combination (woven fabric in thermosetting epoxy resin) and external cross-section dimensions, but different length, wall thickness, laminate stacking sequence and fiber volume content. Simulation works focused on modeling the three modes of collapse (progressive end-crushing with tube wall laminate splaying, local tube-wall buckling and mid-length unstable crushing) observed in the series of static and dynamic compression tests. El-Hage, Mallick and Zamani [11] investigated numerically using LS-DYNA, explicit non-linear finite element software, the quasi-static axial crush performance of aluminum–composite hybrid tubes containing a filament-wound E-glass fiber-reinforced epoxy over-wrap around square aluminum tubes. The fiber orientation angle in the over-wrap was varied between [±30º] and [90º] with respect to the tube's axis. The quasi-static axial crush resistance of the hybrid tubes is compared in terms of the maximum load, mean crush load, crush energy and specific energy absorption. The deformation modes of these tubes are also described. An empirical equation

is proposed for predicting the mean crush force of hybrid tubes. Han et al. [12] carried out a numerical investigation to evaluate the response and energy absorbing capacity of hybrid composite tubes made of unidirectional pultruded tube over wrapped with ±45˚ braided fiber reinforced plastic (FRP). The numerical simulation characterized the crushing behaviors of these tubes subject to both quasi-static compression and axial dynamic impact loadings. Two types of braided FRP, glass and carbon fibers, were considered. Parametric studies were also conducted to examine the influence of the tube's length, thickness and type of braid, as well as the loading conditions on the crushing behavior of the tubes. It was found that braiding over wraps could be used to effectively enhance the crushing characteristic and energy absorbing capability of the tubes.

In the present work, the explicit finite element code LS-DYNA is used to simulate the impact test of a filament-wound square cross section tube, Comparison of the computed compressive response to the experimental work is made. Then a parametric study is conducted to study the effect of inner hole, fiber angle orientation, number of layers (tube thickness) and degree of orthotropy (E_a/ E_b), on the absorbed energy and Specific Energy Absorption of the tube.

Experimental work

The material of the specimens consists of fiber glass roving and polyester resin. The specimens were fabricated by mechanical wet filament winding method using the designed winder seen in Figure (1) which is described in details in reference [13]. The specimens are tubes with square cross section, the inner hole length is (36.3) mm, the thickness is (1.2) mm (two layers [+45º, -45º]) and the length is (100) mm. Specimens preparation was made carefully in order to insure flat smoothed- end surfaces, parallel to each other and at right angles to the length of the specimens so as to prevent localized end failures. Figure (2) shows a photograph of the specimen. The mechanical properties of the specimen material were obtained experimentally using Instron universal testing machine at the laboratories of Production and Metallurgy Engineering Department / University of Technology, are given in table (1).

Impact tests are carried out by means of the designed Drop Weight Tower device, seen in Figure (3) which is described in details in reference [13]. The specimens are placed on the base of the drop weight impact tester at the target area, and impacted by (5 kg) impact weight at an impact velocity of (3.836)m/s, corresponding to drop height of (0.75) m.

Determination of Fiber Volume Fraction (V_f)

The relative quantity of the various constituents in a composite is known as the volume fraction and is normally expressed as the ratio of volume of reinforcement and the total volume of the composite.

Since the experimental procedure for determining the fiber volume fraction is destructive, an analytical procedure is preferred. In determining

the fiber volume fraction analytically, the fiber arrangement in the lamina and the form of the fiber reinforcement in the lamina must be known.

The length of the fiber needed for one winding is limited and scaled, each layer consists of (21) windings. Two layers of windings are used in construction of each pipe, every layer needs (300) cm length of fiber, the weight of fibers was (15.6) gm. The tubes were weighted and the volume fraction of fibers can be calculated using the formula, [14]

$$V_f = \left[1 + \frac{r_g}{r_m}\left(\frac{1}{y} - 1\right)\right]^{-1} \quad \text{.....(1)}$$

where

$y = \frac{W_g}{W_c}$ and V_f : fiber volume fraction

r_g , r_m : fiberglass and matrix density.

y : the weight percent of glass in decimal form, which is the ratio of (W_g) weight of fiberglass to the (W_c) weight of composite tube.

Volume fraction for the tube estimated by calculation is 47%.

Determination of Specific Energy Absorption (SEA)

The most important parameter that was determined from each crush test was the specific energy absorption (SEA), Energy is the product of the force and distance moved at that force level. The total impact energy imparted to a specimen is:

$$E = Mg(h + \Delta L) \quad \text{... (2)}$$

Where (h) is the relative distance between the bottom surface of the impact weight and upper cross section surface of the tube, and (ΔL) is the specimen shortening. (ΔL) is small compared to (h) and is negligible [15].

The mean impact load is

$$(P_m) = \frac{E}{\Delta L} \quad \text{..... (3)}$$

The Specific Energy Absorption was calculated as the mean crush load divided by the mass per unit length of the specimen [16];

$$SEA = P_m\left(\frac{L}{M}\right) \quad \text{.... (4)}$$

Where (M) is the mass and (L) is the length of the tube before crushing.

Finite Element Models Description

The finite element simulation is performed in the usual three typical steps using the basic components of the LS-DYNA code, the first one being the building of the model by means of the internal pre-processor (finite element model building (FEMB)), the second step being the nonlinear dynamic analysis and the final one being the post processor of the analysis result using the POST-GL processor of the LS-DYNA for the interpretation and visualization of the computed data.

LS-DYNA Code

LS-DYNA is a code that was developed by the Lawrence Livermore National Laboratory especially for impact and nonlinear dynamic simulation work.

LS-DYNA is an explicit finite element code, which uses a Lagrangian formulation. The

equations of motion are integrated in time explicitly using central differences. The method requires very small time steps for a stable solution, thus is particularly suitable for impact and crush simulation, and the governing equations do not require global stiffness matrix assembly or inversion [17].

Finite Element Discretization

The specimen geometry with the necessary dimensions and the mesh scheme for the specimen are shown in Figure (4). The element type is Belytshko-Tsay quadrilateral shell element. According to the Belytshko tsay the given thickness is assigned to both side of the element, on this basis the tube is modeled to the dimension of (37.5×37.5) mm, and the wall thickness of (1.2) mm was given at each node for (4) nodded shell elements. The different layers in composite tube are modeled by defining integration point to each layer. The integration points are located evenly through the thickness. The number and locations of the integration point were defined on the SECTION-SHELL and INTEGRATION cards in LS-DYNA. The model of the tube was comprised of total of 2080 elements connected with 2174 nodes.

The impactor was modeled by a planar rigid wall with a mass of (5) kg which is an invisible entity in LS-DYNA. The base at which the specimen was placed during the impact test was modeled by a stationary rigid wall. The rigid walls were defined on the RIGIDWALL-PLANAR cards in LS-DYNA.

Material Model

Assignment of material properties is accomplished via selection of an appropriate material model. LS-DYNA has approximately 100 material models available for use in its data base and the ability to create user-defined material models is also provided. The material model used for modeling of the composite tubes wall was MAT-ENHANCED-COMPOSITE-DAMAGE (MAT 54) as one of most efficient LS-DYNA material models for composites. This material model represent an orthotropic material that behave linearly when undamaged but also allows for nonlinearity through damage parameters as defined by (Chang and Chang) or (Tsai and Wu). The micro failure modes commonly observed in composite laminates are fiber breakage, fiber micro buckling and matrix crushing, transverse matrix cracking, transverse matrix crushing, debonding at the fiber-matrix interface and delamination. The first four failure modes can be treated using thin shell theory, since they depend on in-plane stresses. The debonding failure mode needs three dimensional representation of the constitutive equation and kinematics, and cannot be treated in thin shell theory. The MAT 54 cards are valid only for thin shell element. Laminated shell theory has to be activated in CONTROL- SHELL card, in order to model the transverse shear deformation lamination theory was applied to correct for the assumption of a uniform constant shear strain through the thickness of the shell [18].

The material model (54) has the option of using either the Tsai-Wu failure criterion or the Chang-Chang

failure criterion for lamina failure. The Tsai-Wu failure criterion does not specifically consider the failure modes observed in the composite materials. Chang-Chang failure is separately considered the tensile fiber mode, compressive fiber mode, tensile matrix mode and compressive matrix mode.

Chang and Chang modified the Hashin equation to include the non-linear shear stress – strain behavior of a composite lamina. They also defined the post – failure degradation rule so that the behavior of the laminate can be analyzed after each successive lamina fails.

According to chang and chang criterion, failure of ply subject to tensile fiber loading is assumed whenever the following condition is true [18]:

$$\left(\frac{s_{aa}}{x_t}\right)^2+\beta\left(\frac{t_{ab}}{s}\right)\geq 1 \quad \ldots (5)$$

Where σ_{aa} : stress in longitudinal principle material axis.

τ_{ab} :In-plane shear stress.

χ_t : longitudinal tensile strength.

S : shear strength.

β : weight factor for the ratio $\left(t_{ab}/s\right)$.

For β=1.0 this condition is identical to Hashin failure criteria for the fiber tensile loading, while for β=0 condition (5) corresponds to maximum stress failure criterion. When failure occurs, the material constants E_a (modulus of elasticity in the longitudinal principal material axis), E_b (modulus of elasticity in the transverse principal material axis), G_{ab} (in-plane shear modulus), γ_{ab} (major Poisson's ratio), γ_{ba} (minor Poisson's ratio), are set to zero in the corresponding layer of the composite shell element. In case of compressive fiber modes failure in a ply is assumed whenever the compressive stress (σ_{aa}) reaches the level or exceeds the compressive strength (χ_c) [18].

$$\left(\frac{s_{aa}}{x_c}\right)^2\geq 1 \quad \ldots (6)$$

Similar to the previous case, when failure occurs, material constants E_a ,G_{ab} and γ_{ba} are set to zero in the corresponding layer of the composite shell. Finally regarding the matrix failure, Tsai and Wu failure criterion is adopted for both tensile and compressive matrix modes, i.e. failure is assumed in a ply whenever:

$$\frac{s_{bb}^2}{Y_c Y_t}+\left(\frac{t_{ab}}{s}\right)^2+\frac{(Y_c-Y_t)s_{bb}}{Y_c Y_t}\geq 1 \quad \ldots\ldots (7)$$

Where σ_{bb} :stress in transverse principle material axis.

Y_t :transverse tensile strength.

Y_c : transverse compressive strength.

Same as before, constants E_a , G_{ab} , γ_{ba} , and γ_{ab} are set to zero in the ply of laminate when matrix failure occurs.

A point of particular importance related to material model (54) is the nonlinear stress-strain relation ship adopted for the shear behavior of the modeled composite materials. This consideration uses the following cubic relation:

$$2\varepsilon_{ab}=\frac{t_{ab}}{G_{ab}}+\alpha\tau^{3}_{ab} \quad \dots (8)$$

Where εab: shear strain in a-b plane.

A non-linear shear stress parameter.

Simulation of Contact between Interacting Parts

The contact interface types between the interacting parts of the model are very important. Specifying contact between the parts of the model ensures that the finite element code prevents penetration between the geometric boundaries of the parts during their movement and progressive deformation.

A total of four different types of contact interface were used in the modeling of the impact of the specimens:-

1. The "rigid wall_ Planar" type was used for the contact between the specimen and the stationary rigid platen (base) of the drop weight tester in order to prevent penetration of the boundary of the tester base by the tube specimen's nodes.
2. The"rigid wall planar moving_forces" contact type was used to describe the contact between the tube specimen and the drop weight. A moving rigid wall with a finite mass equal to (5) Kg and an impact velocity equal to (3.836) m/s, represent the impact mass.

From the simulation results related to this rigid wall interface plus the data history for the movement of a mass less node that was specifically assigned to this rigid wall, it was possible to retrieve the required data for generating the load-displacement curve corresponding to the impact tests.

3. The "automatic_sigle_surface" type was used to prevent penetration of the deformed tube boundary by tube's own nodes.
4. The "eroding_single_surface" type was used for the same reason as the previous interface type, but also because the boundary surface of tube was eroded during the compression due to element deletion at the various stages of the tube collapse.

Results and discussion

In following sections, the output of the numerical simulation related to the response and crushing characteristics of the axially compressed tubes is evaluated and compared visually and numerically to the experimental results for the validation of the finite element model.

Visual Comparison of Specimen Folding Pattern

Visual comparison between the folding pattern of the deformed tube specimen of impact test and corresponding image generated by LS-DYNA post processor proves that the finite element simulation approached the features of the collapse mode of the specimen to a satisfactory degree. This is evident when comparing the photograph in Figure (5) to the post-processor image.

Comparison In Terms of Main Crushing Characteristics

To ensure the finite element model was sufficiently accurate it was validated using the experimental results. The tube response obtained by the finite element model was compared with that of experimental

response for a range of crash parameters reported in Table (2).

Parametric Study of Composite Tubes

The following are some of the parameters which were considered for studying the behavior of the composite tubes.

Effect of winding angle (θ)

Figure (6) shows the variation in the absorbed energy with increasing winding angle (θ), for a tube with inner length (36.3) mm, tube thickness (1.2) mm, two layers [+θ, -θ], impacted by (5) kg at an impact velocity (3.836) m/s.

The absorbed energy is decreased by increasing the winding angle until θ = 45º and then increased for still higher angles. Figure (7) shows the variation of SEA with increasing winding angle θ. It can be seen that the SEA increased with the winding angle. The SEA value of the composite tube with winding angle 60º is higher (40.746%) than that with winding angle 20º.

Thornton [19] found that for square cross section tubes of the same thickness, the lay-up sequence, the proportion of 0º layers and the type of trigger can affect the value of SEA. The SEA increased by increasing the proportion of 0º layers for tulip trigger, and decreased by increasing the proportion of 90º layers.

The variation of absorbed energy with winding angle may be attributed to the variation of the stiffness with fiber orientation, as the fiber orientation angle decreased the stiffness increased. The lower SEA has been related to stress concentrations at the corners, which contributes to the formation of splitting cracks and leads to unstable collapse. After the angle 45º the increasing in SEA is due to progressive folding failure mode.

Effect of inner hole length (w_i)

Figure (8) shows the variation in the absorbed energy with increasing inner length w_i from (26.3) mm to (46.3) mm for a tube thickness (1.2) mm, with two layers [+45º, − 45º] impacted by (5) kg at an impact velocity (3.836) m/s. From Figure (8), it can be seen that the absorbed energy is decreased with increasing inner length (w_i). Figure (9) shows the variation of SEA with increasing inner length (w_i). When the inner length increases the SEA decrease. The SEA of the composite tube with inner length (26.3) mm is higher (22.352) % than that with inner length (46.3) mm. The reason for decreasing SEA with increasing the inner length (w_i) is the variation in the failure mode. When the inner length of the tube is small, the tube failed by mixed mode (progressive folding and global buckling), which is the higher absorbed energy with small crushing distance, and higher SEA than the global fracture mode. When the inner length of the tube increases, the tube fails by global fracture mode, which is the lower absorbed energy with large crushing distance and lower SEA.

Effect of tube thickness

Figure (10) shows the effect of increasing the tube thickness on the absorbed energy. The inner length (w_i) is fixed at (36.3) mm, the impact mass is (20) kg while the thickness (number of layers) is gradually increased from (1.8 to 4.2) mm (3 to

7) layers, in the form of [+45º, − 45º, +45º, −...]. This figure shows that the absorbed energy is decreased when the tube thickness is increased. When the tube thickness is small the crushing distance is large then the absorbed energy is large, as the tube thickness increased, the crushing distance decreased and the absorbed energy is small.

The variation of SEA with the tube thickness (t) has shown in Figure (11), when the tube thickness increases the SEA increases. The SEA of the composite tube (4.2) mm thickness is higher (71.977) % than that with (1.8) mm thickness.

A similar crushing behavior was reported by Mc Gregor and et. al. [20] for carbon-fiber/Hetron 922 tubes, it was found that the absorbed energy for single ply tubes is more than four ply tubes, but SEA is increased as the number of plies increased.

The behavior of the composite tubes may be attributed to the stress concentrations at the corners which contributes to the formation of local buckles as tube wall folded, leading to cracking of the tube wall and large crushing distance then less SEA. When the tube thickness increased the failure mode will become unstable mid-length collapse, which is featured by brittle fracture and irregular collapse of the tube that is typically initiated at the middle of the compressed tube with circumferential fracture of the composite tube walls. The crushing distance is small, and then SEA is large.

Effect of degree of orthotropic

Figure (12) shows the variation in the absorbed energy with increasing (E_a / E_b) from 1 to 3 for a tube thickness (1.2) mm, inner length w_i=36.3mm, with two layers [+45º, −45º] impacted by (5) kg at an impact velocity (3.836) m/s.

From Figure (12), it can be seen that the absorbed energy is increased with increasing (E_a / E_b). Figure (13) shows the variation of SEA with increasing (E_a / E_b). It can be seen that the SEA increased with increasing (E_a / E_b). The SEA of the composite tube with (E_a / E_b =3) is higher (30.325) % than that with (E_a / E_b =1).

The reason for increasing of the absorbed energy and SEA with increasing (E_a / E_b), is the effect of (E_a) upon the section rigidity and its ability to resist flexure, also the increasing of axial compressive strength which lead to stable progressive folding failure.

Conclusions

1- LS-DYNA program analysis is able to reproduce satisfactory failure modes that were observed in the experimental works.
2- Reliable modeling of composite tubes crushing response under impact load requires the use of composite material models, such as the enhanced composite damage material model (54) used in this work, in order to adequately model the complex response of a layered fiber reinforced plastic, considering a number of material parameters related to elastic properties and strength.
3- LS-DYNA simulation results pertaining to the main crushing characteristics, such as crushing distance and crash energy

absorption are very close to the experimental results.

4- The specimen geometry and deformation mode played a major role in determining the energy absorption characteristics.
5- The SEA increased with increasing winding angle.
6- Increasing the inner hole of the tube (inner length) decreases the SEA.
7- Increasing the tube thickness (number of layers), increases the SEA.
8- Increasing the degree of orthotropic (E_a / E_b) increases the SEA.

References

[1]Mahdi, E., Hamouda, A. M.S., Sahari, B. B. and Khalid,Y.A., "Experimental quasi-static axial crushing of cone-tube-con composite system", composite: Part B 34 (2002) 285-302.

[2]Goetzen, W.K. and Kessler, M.R., :Dynamic mechanical analysis of carbon/epoxy composites for structural pipeline repair", Composites: Part B 38 (2007) 1-9.

[3]Tarlochan, F., Hamouda, A.M.S.,Mahdi, E., Sahari, B.S., "On the compression behavior of thin walled polymer composite sandwich panels" The 3rd International Conference on Structural Stability and Dynamics June 19-22, 2005, Kissimmce, Florida.

[4]Hull,D."A Unified Approach to Progressive Crushing of Fibre Reinforced Composite Tubes," Composite Science and Technology, Vol. 40, 1991, pp. 377-421.

[5]Shin, Kum Cheol, Lee, Jung Ju, Kim, Ku Hyun, Song, Min Cheol and Huh, Jeung Soo, "Axial crush and bending collapse of an aluminum/GFRP hybrid square tube and its energy absorption capability", Composite Structures 57 (2002) 279–287.

[6]Mahdi, E, Hamouda, A. M. S., Sahari, B. B. and Khalid, Y. A., "On the Collapse of Cotton / Epoxy Tibes under Axial Static Loading", Journal of Applied Composite Materials, 10: 67-84, 2003.

[7]Zeng, Tao, Fang, Dai-ning, and Lu, Tian-jian, "Dynamic Crashing and Impact Energy Absorption of 3D Braided Composite Tubes", Materials Letters 59; 1491-1496, 2005.

[8]Mamalis, A.G Manolakos, D. E., Ionnidis, M. B., and Papapostolou,O.P., "On The Response of Thin-Walled CFRP Composite Tubular Components Subjected to Static and Dynamic Axial Compressive Loading: Experimental", Composite Structures, Vol. 69, pp407-420, 2005.

[9]Al-Badrany, Ayad Aied Mahuof, "Energy Absorption Capacity of Thin Metalic Tubes," Ms.c. thesis University of Al-Anbar, Iraq, 2005.

[10]Mamalis, A.G., Manolakos, D.E., Ioannidis, M.B., and Papapostolou, D. P., "The Static and Dynamic Axial Collapse of CFRP Square Tubes:Finite Element Modeling", Composite Structures, 74:213-225, 2006.

[11] El-Hage, H., Mallick, P. K. and Zamani, N., "A numerical study on the quasi-static axial crush characteristics of square aluminum–composite hybrid tubes", Composite Structures 73 (2006) 505–514.

[12] Han, Haipeng, Taheri, Farid, Pegg, Neil, and Lu, You, "A Numerical Study on The Axial Crushing Response of Hybrid Pultruded and ±45º Braided Tubes", Composite Structure, 80; 235-264, 2007.

[13]Wahaib, Mohammad Abdul-Hassan, "Buckling Deformation of Composite Materials Under Impact Axial Loading at Elevated Temperature" Ph. D. thesis, Electromecanical Engineering Department/U.O.T Iraq, 2009.

[14]K., Geof, "Design and Manufacture of Composite Structures", McGraw Hill Inc., 1994.

[15]Song, Hong-Wei, Wan, Zhi-Min, Xie, Zhi-Min, and Du, Xing-Wen, "Axial Impact Behavior and Energy Absorption Efficiency of Composite Wrapped Metal Tubes", International Journal of Impact Engineering, Vol. 24 pp 385-401, 2000.

[16]Silcock, M., Hall, W., Fox, B., and Warrior, N., "Finite Element Modeling of Metallic Tubular Crash Structures With an Explicit Code", Int. J. Vehicle Safety, Vol. 1, No. 4, pp 292-303, 2006.

[17]LS-DYNA Keyword User's Manual, V 971, Livermore Software Technology Corporation, Livermore, U.S.A., 2005.

[18]Hallquist, J., "LS-DYNA Theoretical Manual", Livermore Software Technology Corporation, Livermore, U.S.A, 2005.

[19]Thornton, P.H., "The Crush Behavior of Glass Fiber Reinforced Plastic Sections", Composite Science and Technology, 27 (1986) 199-223.

[20]Mc, Gregor, Carla J., Vaziri, Reza, Poursartip, Anoush and Xiao, Xinran, "Simulation of progressive damage development in braided composite tubes under axial compression", Composites: Part A 38 (2007) 2247-2259.

Figure (1) The winding machine

Figure (2) photograph of the specimen

Figure (3) The Drop Weight Impact Tester

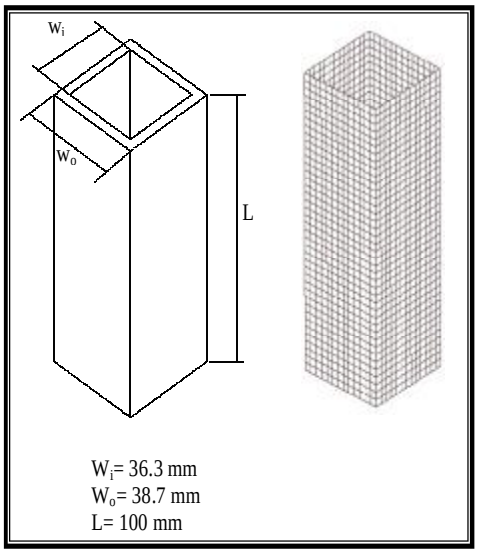

Figure (4) Discretization of specimen

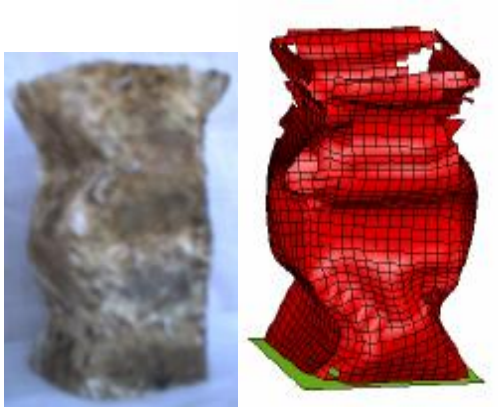

Figure (5) Comparison between experimental and theoretical collapse Mode

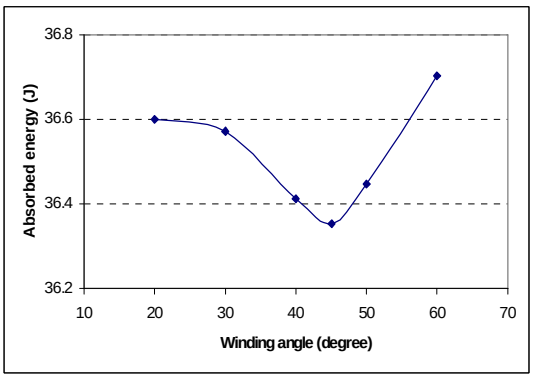

Figure (6) Variation in absorbed energy with winding angle

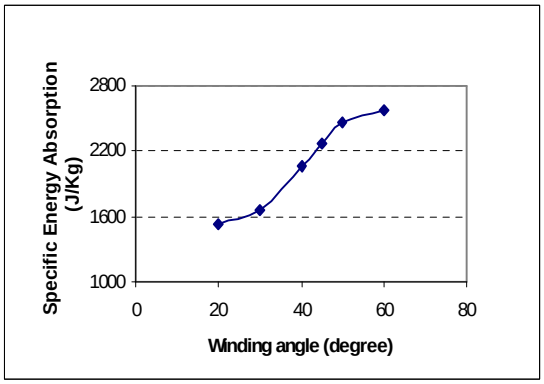

Figure (7) Variation of SEA with winding angle

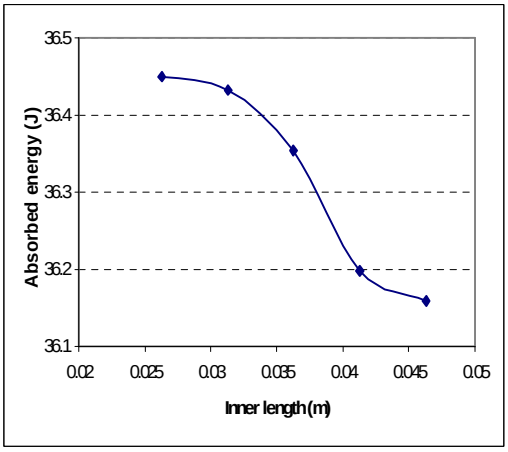

Figure (8) Variation in absorbed energy with increased inner length (w_i)

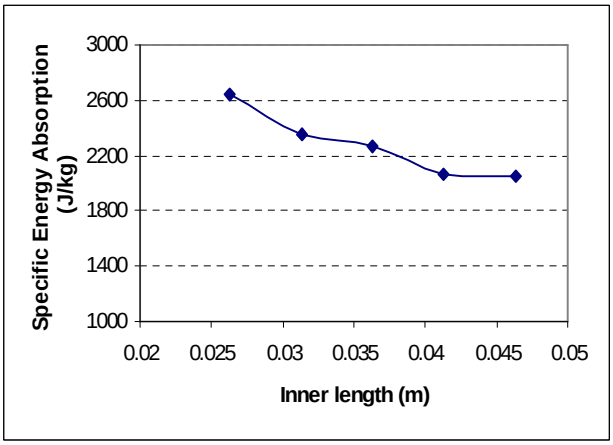

Figure (9) Variation of SEA with increased inner length (w_i)

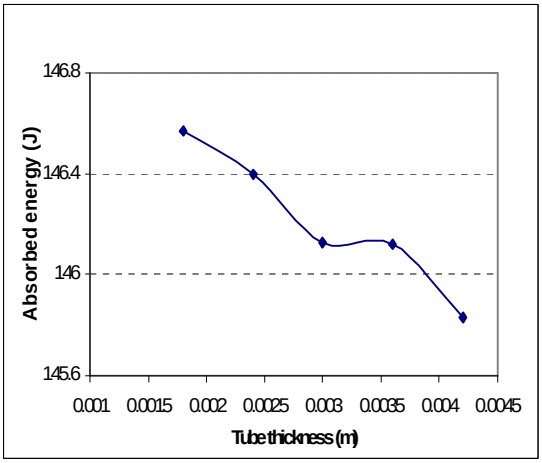

Figure (10) Variation of absorbed energy with increased tube thickness for an inner length wi=36.3 mm

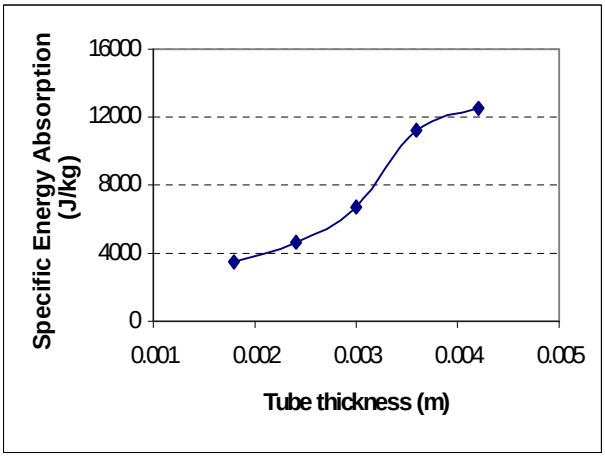

Figure (11) Variation of Specific Energy Absorption with increased tube thickness for an inner length wi=36.3 mm

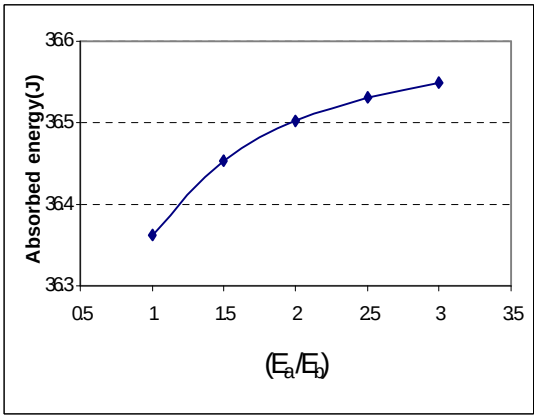

Figure (12) Variation of absorbed energy with increased (E_a / E_b).

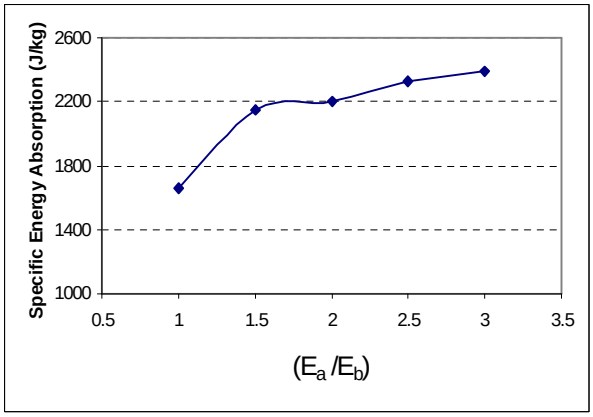

Figure (13) Variation of SEA with increased (E_a / E_b)